

Equilibrium and Dynamics of Soluble Surfactant Penetration into a Langmuir Monolayer of a 2D Aggregating Homologue

V. B. Fainerman,[†] A. V. Makievski,^{†,‡} D. Vollhardt,^{*,‡} S. Siegel,[‡] and R. Miller[‡]

Institute of Technical Ecology, 25 Shevchenko blvd., 340017, Donetsk, Ukraine, and Max-Planck-Institut für Kolloid- und Grenzflächenforschung, Rudower Chaussee 5, D-12489, Berlin-Adlershof, Germany

Received: July 7, 1998; In Final Form: November 9, 1998

The penetration dynamics of a dodecyldimethylphosphine oxid dissolved in the aqueous substrate into a Langmuir monolayer of eicosanyldimethylphosphine oxide and the equilibrium characteristics of the mixed monolayer formed are experimentally and theoretically studied. For the theoretical description of the low-density gaseous monolayers, the generalized Szyszkowski–Langmuir equation of state and the adsorption isotherm equation were applied. After the main phase transition, at which the gaseous phase starts to coexist with a condensed phase as a result of 2D aggregation, the monolayers are considered within the framework of a generalized Volmer equation and a quasichemical model for the aggregational equilibrium. The equations of state for the mixed monolayer are derived corresponding to different assumptions about the composition of 2D aggregates. The adsorption isotherm equations for soluble surfactant within the tightly packed monolayer are derived from the simultaneous solution of the corresponding equations of state and Pethica's equation. For the mixture of insoluble eicosanyldimethylphosphine oxide and soluble dodecyldimethylphosphine oxide, the experimental results were shown to agree well with the theoretical predictions based on the characteristics of these surfactants in the single-component solutions and monolayers. The model based on mixed aggregates is best suited to match the experimental values both for Π – A and Π – t isotherms.

Introduction

Mixed monolayers that consist of insoluble and soluble amphiphiles at the air/solution interface are interesting models for studying the penetration of insoluble monolayers by a soluble surfactant or protein. For decades there is a wide variety of biophysical, biotechnological, and biomedical motivations for studying such systems. Numerous papers on the equilibrium behavior of penetrated monolayers have been published.^{1–12} In a fundamental paper of Hall¹³ the penetration is analyzed with the Gibbs's equation, which gives the definitive rigorous formal thermodynamic statement of monolayer penetration. He concluded that it is impossible to obtain the surface density of the penetrating species from surface pressure–concentration data. His method did not result in an equation of state for penetrated monolayers.

On the basis of physically reasonable assumptions, Pethica proposed an adsorption equation that describes the monolayers composed of one soluble and one insoluble surfactant.¹ Pethica's equation was generalized for the case that the monolayer consists of different species—either soluble or insoluble amphiphilic molecules.¹⁴ The generalized Pethica equation was analyzed thermodynamically.^{15,16}

Further equations were proposed to describe equilibrium penetration.^{3–8} Some known theoretical approaches were analyzed with the conclusion that penetration theories proposed so far are applicable for a rather narrow range of systems.^{11,12} In most cases, the penetration theories are incapable of providing analytical expressions for equations of state of mixed monolayers and adsorption isotherms of soluble surfactants. For

example, a theoretical analysis for the important case of a 2D phase transition within the amphiphilic monolayer where a soluble surfactant is also present, has not been performed up to now. Only few studies dealing with the dynamics of the penetration process were published.^{9,10} This problem clearly is more involved theoretically than the description of the penetration equilibrium.

The present work is focused on both the theoretical and experimental study of a rather simple system, which consists of the mixed monolayer of an insoluble ($C = 20$) and soluble ($C = 12$) homologue of dimethylphosphine oxide. As the values of partial molar area of the two homologues are roughly equal, and the adsorption layer of soluble surfactant exhibits an ideal behavior, the theoretical analysis of equilibrium and dynamic behavior of mixed monolayer has simplified significantly. The surface pressure–area (Π – A) isotherms of the insoluble homologous dimethylalkylphosphine oxides with $C \geq 20$ undergo a first-order phase transition, i.e., a two-dimensional aggregation at compression. This was supported by studies using Brewster angle microscopy (BAM) and X-ray diffraction at grazing incidence (GIXD); their results will be presented in another paper.¹⁷ In the present paper, we show that, on the basis of the generalized Volmer's equation, both the effect of a soluble component on the characteristics of the aggregation equilibrium and the effect of aggregation on the penetration rate and the dynamics of the surface pressure increase of the mixed monolayer can be analyzed.

Theory

Equilibrium. The equation of state for ideal adsorption layers, which consists of i homologous amphiphiles with nearly the same values of partial molar area ω_i , can be presented in the

* Corresponding author.

[†] Institute of Technical Ecology.

[‡] Max-Planck-Institut für Kolloid- und Grenzflächenforschung.

form of the generalized Szyszkowski–Langmuir equation of state^{15,16}

$$\Pi = -\frac{RT}{\omega} \ln(1 - \sum_{i \geq 1} \Theta_i) \quad (1)$$

where R is the gas constant, T is the temperature, $\Pi = \sigma_0 - \sigma$ is the surface pressure, σ_0 and σ are the surface tensions of solvent and solution, respectively, $\Theta_i = \Gamma_i/\Gamma_\infty$ is the coverage of the monolayer, Γ_∞ is the limiting adsorption value ($\Gamma_\infty = 1/\omega$), and Γ_i is the adsorbed amount of the i th component. The adsorption isotherm for the i th component of the system can be represented in form of the generalized Langmuir equation^{15,16}

$$b_i c_i = \frac{\theta_i}{(1 - \sum_{i \geq 1} \theta_i)} \quad (2)$$

where b_i is the adsorption equilibrium constant and c_i is the bulk concentration of the i th component. The equation of state (eq 1) remains also valid in the case where the insoluble homologues are present within the surface layer along with the soluble homologues, provided that the Θ_i values for the insoluble components are not too high. In this case, eq 2 remains also valid for the soluble components of the system, see ref 8. It follows that the value of Γ will as referred to be the surface concentration with respect to both soluble and insoluble components. Note, however, that for insoluble components this value is equal to the total two-dimensional molar density of the component, not the excess density. For a mixture of k soluble and s insoluble components it is convenient to express eq 1 in the form of Krotov's equation¹⁵

$$\Pi = \frac{RT}{\omega} \ln \left(\frac{1 + \sum_{i=1}^k b_i c_i}{1 - \sum_{j=1}^s \theta_j} \right) \quad (3)$$

For the case of a single soluble surfactant in the presence of a single insoluble component within the surface layer, eq 3 can be simplified to

$$\Pi = \frac{RT}{\omega} \ln \frac{(1 + bc)}{(1 - \Theta_2)} \quad (4)$$

where the subscripts 1 and 2 refer to the soluble surfactant and the insoluble component, respectively. The adsorption isotherm equation for the soluble component becomes

$$\Gamma_1 = \Gamma_\infty (1 - \Theta_2) \frac{bc}{1 + bc} \quad (5)$$

As mentioned above, eqs 4 and 5 are valid if the Θ_2 values are relatively small with respect to the Θ_1 values. These equations lead to two important conclusions. The first is that it follows from eq 4 that the surface pressure changes that arise due to the adsorption of the soluble surfactant, i.e., the surface pressure difference between the mixed monolayer and the insoluble monolayer $\Delta\Pi$, do not depend on Θ_2 but rather on the value of the product bc , $\Delta\Pi = (RT/\omega) \ln(1 + bc)$. The second is that according to the isotherm equation eq 5, in the presence of the insoluble component the monolayer coverage by the soluble component $\Theta_1 = \Gamma_1/\Gamma_\infty$ decreases proportionally to $(1 - \Theta_2)$.

Therefore, the Θ_1 value, which corresponds to the $\Delta\Pi$ value of the mixed monolayer, is lower than the Θ_1 value of the same $\Delta\Pi$ value when the monolayer does not contain an insoluble amphiphile. It will be shown below that this behavior can result in a more rapid achievement of the adsorption equilibrium in the case when an insoluble amphiphile is present.

The system can be described by the generalized Volmer equation¹⁸ when the Θ_2 value is comparatively high, while the Θ_1 value is small

$$\Pi = RT \frac{\sum_i \Gamma_i}{1 - \sum_i \Gamma_i \omega_i} - B \quad (6)$$

where $B = \text{const} = \Pi^*$ is the cohesion pressure. It can be seen that eq 6 accounts for the nonideality of the surface layer. The adsorption isotherm equation for the soluble components of the system can be derived from the simultaneous solution of eq 6 and the generalized Pethica equation^{14,16}

$$\left(\frac{\partial \Pi}{\partial \ln c_j} \right)_{\Gamma_{i \neq j} = \text{const}} = RT T_j [1 - \sum_{i \neq j} \Theta_i]^{-1} \quad (7)$$

For the case where two amphiphiles exist, one obtains

$$bc = \left(\frac{\theta_1}{1 - \theta_1 - \theta_2} \right)^{1/(1-\theta_2)} \exp \left[\frac{\theta_1}{(1 - \theta_2)(1 - \theta_1 - \theta_2)} \right] \quad (8)$$

It can be easily shown that eq 2 also follows from the simultaneous solution of eqs 1 and 7.

The equation of state eq 6 can be generalized to describe the formation of a condensed phase, i.e., of two-dimensional aggregates within the monolayer.

Assuming that mixed aggregates can exist, one obtains

$$\Pi = RT \frac{\Gamma_{11} + \Gamma_{21} + \Gamma_a}{1 - \omega(\Gamma_{11} + \Gamma_{21} + n\Gamma_a)} - B \quad (9)$$

where the second subscript “1” refers to monomers, Γ_a is the surface concentration of aggregates, and $n = n_1 + n_2$ is the total aggregation number for both the soluble and the insoluble component. From the quasichemical model of aggregation,¹⁹ the relation between the molar ratio x of aggregates and monomers, existing within the monolayer, follows

$$x_a = K_a x_{21}^{n_2} x_{11}^{n_1} \quad (10)$$

where K_a is the constant of the aggregation equilibrium. Setting next $x_{11} = bx_{21}$, and introducing Γ_a instead of the molar ratios (which is rigorous enough, because ω is constant for both components), one obtains

$$\Gamma_a = K b^{n_1} \Gamma_{21}^{n_1} \quad (11)$$

According to ref 20, the constant K can be expressed via the critical surface concentration of aggregation of the insoluble amphiphile Γ_{2c}

$$K = (\Gamma_{21}/\Gamma_{2c})^{n-1} \quad (12)$$

Then eqs 11 and 12 yield

$$\Gamma_a = b^{n_1} \Gamma_{21}^n \left(\frac{\Gamma_{21}}{\Gamma_{2c}} \right)^{n_2+n_1-1} \quad (13)$$

Introducing this expression into eq 9, one obtains the most general equation of state for a surface layer composed of two amphiphiles. Note that for a compressible monolayer containing a soluble surfactant, the condition $b = \text{const}$ is valid for its desorption, which is shown below to be the case for the system considered.

Now some particular cases of eq 9 can be examined. Consider first the penetration of the soluble component into the gaseous monolayer of the insoluble component 2. This process occurs at relatively low Θ_2 values. Provided the penetration does not result in the formation of aggregates, one obtains from eq 9 or 6 the equation of state for the two-component mixed surface layer

$$\Pi = RT \frac{\Gamma_1 + \Gamma_2}{1 - \omega(\Gamma_1 + \Gamma_2)} - B \quad (14)$$

Next eq 14 can be transformed in order to describe the situation that the mixed monolayer undergoes compression after the penetration process is completed. If neither desorption of the soluble component nor an aggregation process occurs, the equation that describes the balance of component 1 within the monolayer, $\Gamma_1 = \Gamma_{10}(A_0/A)$, can be applied, where Γ_{10} is the adsorption of component 1 corresponding to the value A_0 of the monolayer area per one molecule of the insoluble component and A , the current value of monolayer area per one molecule of the insoluble amphiphile. Noting that $\Gamma_2 = 1/A$, one obtains

$$\Pi = RT \frac{\Gamma_{10}A_0 + 1}{A - \omega - \Gamma_{10}A_0\omega} - B \quad (15)$$

The value Γ_{10} entering this equation can be calculated from eq 5, which is convenient to convert into the form

$$\Gamma_{10} = \left(\frac{1}{\omega} - \frac{1}{A_0} \right) \frac{bc}{1 + bc} \quad (16)$$

The equation of state valid for the 2D transition region will be first derived for the case when the molecules of the soluble surfactant do not enter the 2D aggregates, i.e., assuming $n_1 = 0$ and $n_2 \gg 1$. The relations valid for large aggregation numbers ($\Gamma_{21} \cong \Gamma_{2c}$, $\Gamma_a \cong 0$, and $n_2\Gamma_a \cong \Gamma_2 - \Gamma_{2c}$) derived in ref 19 from the analysis of eq 13 can be used to transform eq 9 into the expression

$$\Pi = RT \frac{\Gamma_1 + \Gamma_{2c}}{1 - \omega(\Gamma_1 + \Gamma_2)} - B \quad (17)$$

Introducing next the values of area per one molecule of the insoluble surfactant, one obtains

$$\Pi = RT \frac{\Gamma_{10}A_0 + A/A_{2c}}{(A - \omega) - \Gamma_{10}A_0\omega} - B \quad (18)$$

where $A_{2c} = 1/\Gamma_{2c}$ is the monolayer area per one molecule of the component 2, corresponding to the start of 2D aggregation within the insoluble monolayer. The existence of soluble surfactant within the monolayer can possibly lead to an increase of the A_{2c} value, because an additional surface pressure exerted by these molecules promotes the aggregation of the insoluble

molecules. This conclusion follows also from eq 10, which shows that the increase in the ratio of component 1 leads to the increase in the concentration of the aggregates. It is easily seen that if a soluble surfactant is absent, eq 18 can be transformed into the expression recently derived for the 2D transition region in¹⁹

$$\Pi = RT \frac{A/A_{2c}}{A - \omega} - B \quad (19)$$

If mixed aggregates can be formed, and the conditions $n_1 \gg 1$ and $n_2 \gg 1$ hold, it follows from eqs 9 and 13 that

$$\Pi = RT \frac{\Gamma_{1c} + \Gamma_{2c}}{1 - \omega(\Gamma_1 + \Gamma_2)} - B \quad (20)$$

where Γ_{1c} is the surface concentration of the soluble component 1 corresponding to the start of the 2D transition of component 2. Similarly to Γ_1 , this value has to be calculated by assuming possible compression of the monolayer at $A < A_0$. Transforming eq 20, one obtains

$$\Pi = RT \frac{(\Gamma_{10}A_0 + 1)A}{A_{2c}[(A - \omega) - \omega\Gamma_{10}A_0]} - B \quad (21)$$

Similarly to eq 18, for $\Gamma_1 = 0$ this expression yields also eq 19. It follows from eq 18 that the adsorption of the soluble component causes an increase of the monolayer surface pressure throughout the whole range of A values. The shape of the Π - A isotherm changes due to the fact that an additional (as compared with eq 19) term $\Gamma_{10}A_0$ enters the numerator in the right-hand side of eq 21. In the plateau region of the Π - A isotherm with $A < A_c$, a weak dependence of Π on A , which is common for a 2D transition, becomes more steep, and the increase of the slope becomes more pronounced with the increase in the adsorption of soluble surfactant. Equation 21, in addition to eq 18, predicts also an increase of the surface pressure throughout the whole A range. In contrast to eq 18, however, the shape of the Π - A isotherm determined by eq 21 is less steep. Therefore, based on the shape of the Π - A isotherms of the mixed monolayer, it is possible to distinguish between the case when the formation of mixed aggregates occur and that when the aggregates consists only of insoluble amphiphiles.

Dynamic Surface Tension. We next proceed with the discussion of the penetration kinetics of component 1 into the insoluble monolayer, and the variation in surface pressure jump $\Delta\Pi$ determined by this penetration process. The well-known integro-differential equation derived by Ward and Tordai²¹ is the most general relationship between the dynamic adsorption $\Gamma(t)$ and the subsurface concentration $c(0,t)$ for fresh nondeformed surfaces

$$\Gamma = 2\sqrt{\frac{D}{\pi}} [c\sqrt{t} - \int_0^{\sqrt{t}} c(0,t-\lambda) d\sqrt{\lambda}] \quad (22)$$

where D is the diffusion coefficient, t is the time, and λ is a dummy integration variable. Equation 22 is valid for nondiffusion, mixed, and pure diffusion-controlled adsorption mechanisms. In the latter case, the adsorption isotherm is an additional equation between the adsorption and the subsurface concentration. Equation 22 can also be clearly applied to describe the penetration of a Langmuir monolayer. For the diffusion mechanism of the penetration process, the relation between subsurface concentration and adsorption is given by the isotherm equation (eq 5) in the region where 2D aggregation does not occur. The

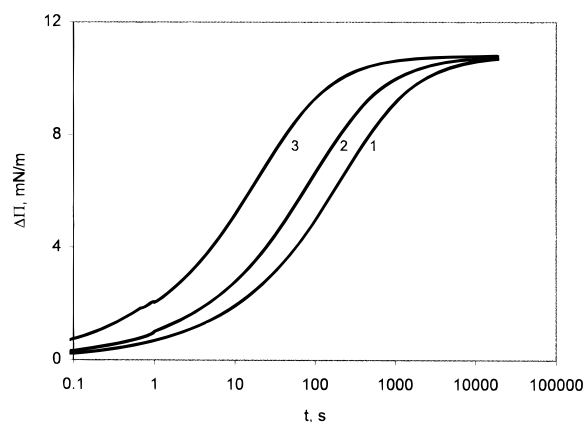


Figure 1. Dynamic surface tension of monolayers for $\Theta = 0$ (curve 1), 0.35 (curve 2), and 0.7 (curve 3) due to the adsorption of the soluble surfactant. The curves are calculated from eqs 22, 23, and 5 for $c = 10^{-5}$ mol/L, $D = 5 \times 10^{-6}$ cm²/s, $\Gamma_{\infty} = 4.39 \times 10^{-10}$ mol/cm² ($\omega = 2.28 \times 10^9$ cm²/mol), and $b = 1.69 \times 10^5$ L/mol.

simultaneous numerical solution of eqs 22 and 5 was performed using the collocation method described previously.²² The variation of the dynamic surface pressure caused by the penetration of the insoluble amphiphilic monolayer by a soluble surfactant can be calculated using the equation

$$\Delta\Pi = \frac{RT}{\omega} \ln(1 + bc(0,t)) \quad (23)$$

which follows from eq 4. The results of the calculations performed for a single value of bulk concentration of soluble surfactant and various values of monolayer coverage by insoluble surfactant are presented in Figure 1. It can be seen that the increase of Θ_2 leads to a decrease in the time necessary to achieve the equilibrium state, and to a significant increase of $\Delta\Pi$. As mentioned above, this phenomenon is caused by a decrease in the equilibrium adsorption value for a soluble surfactant in the presence of an insoluble amphiphile.

Materials and Methods

The alkyldimethylphosphine oxides (C_n DMPO) with various alkyl chain lengths ($n = 12$ and 20) were prepared by V. Yu. Popov, Institute of Organic Chemistry, Ukrainian Academy of Sciences, Donetsk, Ukraine. The chemical purity of the long chain phosphine oxides ($\geq 99\%$) was checked by elemental analysis and HPLC. To avoid the effect of surface-active impurities on the adsorption data, the phosphine oxides were additionally purified by an adsorptive purification procedure. According to this procedure, all impurities having a higher surface activity than the main component are removed from the aqueous solution by a defined stream of nitrogen bubbles.²³ The surface chemical purity of the phosphine oxides was concluded from a special procedure of the adsorption kinetics.²⁴ Ultrapure water having a specific resistance of 18.2 M Ω cm was obtained with a Millipore desktop unit. Its surface tension measured at 20 °C was 72.75 mN m⁻¹. The surface tension measurements of soluble dodecyldimethylphosphine oxide were performed at 20 °C using the tensiometers TVT1 (drop volume method) and TE1 (ring method) from Lauda, described in detail elsewhere.^{25–28} As the time ranges of the methods partially overlap, the full dynamic curves were measured for all the systems studied and the equilibrium surface tensions obtained by extrapolation to infinite time. The experimental results obtained by the TVT1 device were represented as the dependence of the dynamic surface tension on the so-called effective

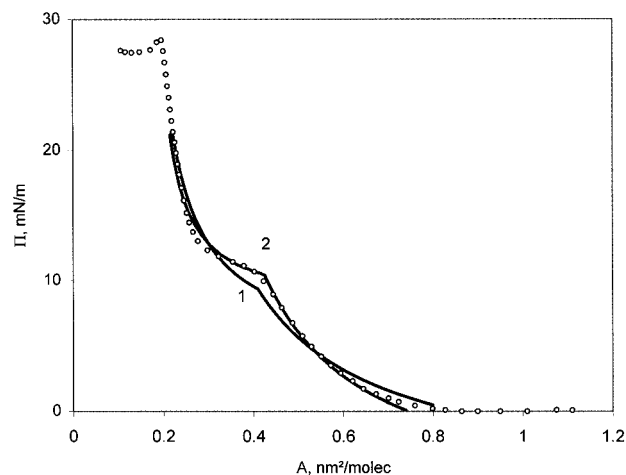


Figure 2. Π - A isotherm of the C_{20} DMPO monolayer ($T = 20$ °C): (curve 1) calculated from eq 19 for $\omega = 0.14$ nm²/molecule, $A_{c2} = 0.41$ nm²/molecule, and $B = 5.6$ mN/m; (curve 2) calculated from eq 24 for $\omega = 0.2$ nm²/molecule, $A_{c2} = 0.42$ nm²/molecule, $B = 7.4$ mN/m, and $\epsilon = 0.15$; (○) experiment.

time t , i.e., reduced to the nondeformed plane surface. The effective time was calculated from the physical time, corrected both for the expansion of the surface and for the radial flow of the liquid within the drop and outside the bubble.²⁵ For the drop volume method, the hydrodynamic effects characteristic of a short time range were also taken into account.²⁹

A circular trough apparatus described in detail elsewhere¹¹ was used for performing the characterization of the Langmuir monolayer of eicosanyldimethylphosphine oxide (C_{20} DMPO) and the penetration of the soluble dodecyldimethylphosphine oxide (C_{12} DMPO) into the monolayer of insoluble C_{20} DMPO.

The principle of the procedure for the penetration studies consists of moving the Langmuir monolayer enclosed between two barriers over at least two segments of the multicompartment trough. The experiments were performed as follows. The circular trough was partitioned only into two semicircular halves by two fixed segment boundaries. At the surface of one region the monolayer was formed by spreading of C_{20} DMPO dissolved in a heptane/ethanol mixture (9:1). The other isolated region of the Langmuir trough was filled with C_{12} DMPO solution with a predefined concentration. The Langmuir monolayer was then compressed by a movable barrier until a predefined value of the area per C_{20} DMPO molecule was achieved. Afterward the monolayer enclosed between the two radial barriers was swept by a simultaneous movement of the barriers to the region containing the C_{12} DMPO solution. The movement of the monolayer was rapid enough (10 s or less) and it took not more than 20 s to stabilize the pressure indications. During the movement, the surface of the C_{12} DMPO solution was cleaned by the barrier that confined the insoluble monolayer. Therefore, the surface layer in its initial state contained no soluble surfactant. In test experiments with monolayer transfer to a pure aqueous subsolution, the pressure difference had not exceeded 0.5 mN/m. During the penetration process, the variation of the surface pressure with time was recorded. When the adsorption equilibrium was established, expansion/compression deformations of the mixed monolayer were performed with simultaneous measurements of the surface pressure and the area per one C_{20} -DMPO molecule.

Results and Discussion

Figure 2 shows the surface pressure–area (Π - A) isotherm of the C_{20} DMPO monolayer at 20 °C recorded with a compres-

sion rate of 0.06 nm²/molecule min. In fact, this isotherm corresponds to the equilibrium state, as a 2–3 times decrease in the compression rate did not affect its position and shape. The existence of a nonhorizontal plateau region with an inflection point at $A \approx 0.4$ nm²/molecule of the Π – A isotherm at lower area values indicates that a two-phase coexistence region exists and aggregates of a condensed two-dimensional C₂₀DMPO phase are formed.

The experimental isotherm shown in Figure 2 can be described satisfactorily by a simple theoretical model presented in ref 20 and eq 19 therein. However, the value $\omega = 0.14$ nm²/molecule estimated from the best fit to the experimental data seems to be unrealistic, as it is seen from Figure 2 that the tightest molecular packing is approximately 0.2 nm²/molecule. Therefore, for processing the experimental data we have also used a more rigorous theory,^{30,31} which in contrast to eq 19, involves the dependence of the monomer surface concentration on the monolayer area ($\Gamma_{2c} \approx A/A_{2c}$), and the possibility that the molecular area of the monomer within the aggregate can differ from ω , that is, $\omega_n = n\omega(1 - \epsilon)$. This theory yields, instead of eq 19, a more complicated equation of state for Langmuir monolayers³⁰

$$\Pi = \frac{RT(A/A_{2c})^2 \exp(-2\Delta\Pi\epsilon\omega/RT)}{A - \omega\{1 + \epsilon[(A/A_{2c})^2 \exp(-2\Delta\Pi\epsilon\omega/RT) - 1]\}} - B \quad (24)$$

where $\Delta\Pi = \Pi - \Pi_c$ and Π_c is the surface pressure at $A = A_{2c}$. The values calculated from eq 24 are also shown in Figure 2. It is seen that a good agreement exists between the new theory and the experimental data for both the gaseous and the condensed state of the C₂₀DMPO monolayer with quite realistic parameter values, which enter into eq 24 estimated from the fitting program, $\omega = 0.2$ nm²/molecule and $\epsilon = 0.03$. Note that $\epsilon = 0.15$ means that the area per one molecule within the aggregate is 15% lower than that for nonaggregated molecules. If the value $\epsilon = 0$ is used, the agreement between the theory and experiment deteriorates slightly for $A < 0.25$ nm²/molecule.

The studies of the penetration process of the soluble C₁₂DMPO molecules into C₂₀DMPO monolayer and the subsequent compression of the mixed monolayer were performed for some fixed initial values of area per one C₂₀DMPO molecule: $A_0 = 0.6$ nm²/molecule (gaseous monolayer), $A_0 = 0.35$ nm²/molecule (2D aggregation region), $A_0 = 0.22$ nm²/molecule (condensed monolayer near the collapse point). The results obtained for $A_0 = 0.6$ nm²/molecule and a 10^{−5} M C₁₂DMPO solution are presented in Figures 3 and 4. Figure 3 shows the isotherm for initial compression of the monolayer to $A_0 = 0.6$ nm² (curve 1) and the mixed monolayer compression isotherm after the adsorption equilibrium was established (curve 2). Figure 4 illustrates the C₁₂DMPO penetration dynamics for $A_0 = 0.6$ nm²/molecule.

Consider first the dynamics and the equilibrium of the penetration into a gaseous monolayer at different C₁₂DMPO concentrations. Figure 5 shows the surface pressure isotherms of a C₁₂DMPO solution for a purified water surface and for the case when a C₂₀DMPO monolayer is present at $A_0 = 0.6$ nm²/molecule, i.e., for $\Theta_2 = 0.35$. The theoretical isotherm for the C₁₂DMPO adsorption at the purified surface was calculated from the Szyszkowski equation $\Pi = (RT/\omega) \ln(1 + bc)$, while eq 4 was used for the mixed monolayer. In both cases the same parameter values were assumed: $\omega = 2.28 \times 10^9$ cm²/mol and $b = 1.69 \times 10^5$ L/mol. The surface pressure isotherm for aqueous C₁₂DMPO solutions corresponds well to the Szysz-

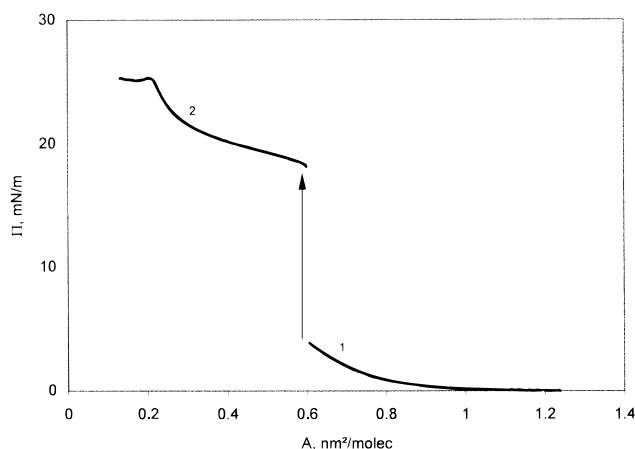


Figure 3. Π – A isotherm of the C₂₀DMPO monolayer ($T = 20$ °C): (curve 1) initial compression of the monolayer to $A_0 = 0.6$ nm²/molecule; (curve 2) mixed monolayer compression isotherm.

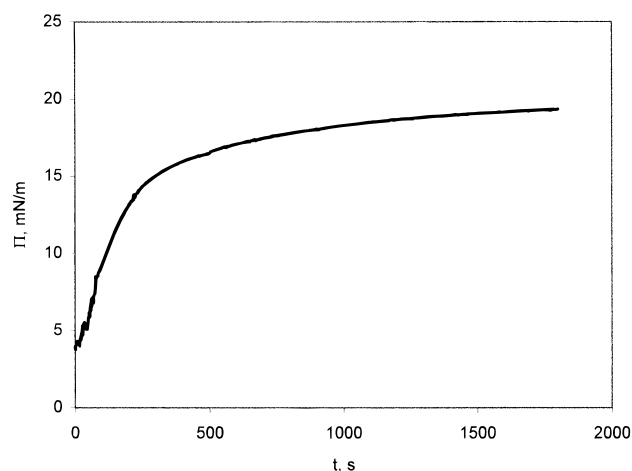


Figure 4. C₁₂DMPO penetration dynamics for $c = 10^{-5}$ mol/L and $A_0 = 0.6$ nm²/molecule.

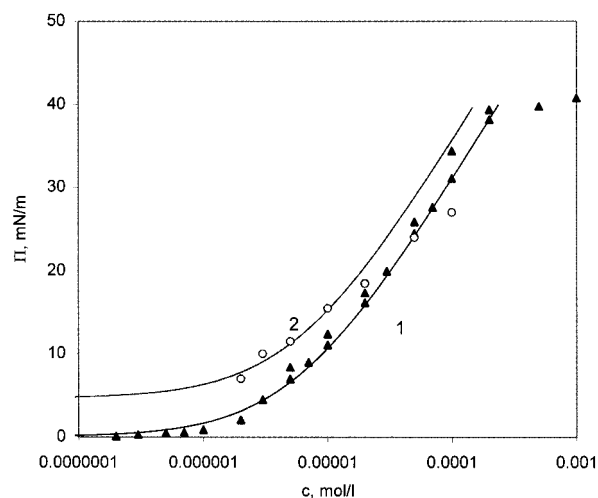


Figure 5. Surface pressure isotherm for C₁₂DMPO solutions at $\Theta_2 = 0$ (curve 1, theory; \blacktriangle , experiment) and $\Theta_2 = 0.35$ (curve 2, theory; \circ , experiment). Theoretical curves calculated with $\omega = 2.28 \times 10^9$ cm²/mol and $b = 1.69 \times 10^5$ L/mol.

kowski equation. Therefore, the concept, which assumes an ideal surface layer for the soluble surfactant, is applicable to the system studied. It is seen that for a mixed monolayer there also exists a satisfactory agreement between the theory and the experiment at $c \leq 10^{-5}$ mol/L. For higher C₁₂DMPO concentrations, however, the experimental Π values are significantly

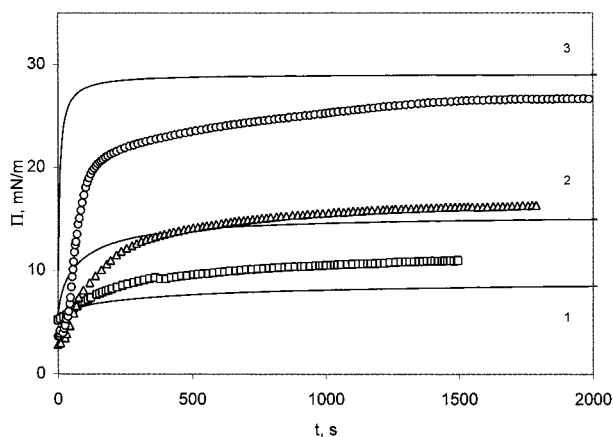


Figure 6. C_{12} DMPO penetration dynamics for $\Theta_2 = 0.35$ and $c = 3 \times 10^{-6}$ mol/L (curve 1, theory; \square , experiment), $c = 10^{-5}$ mol/L (curve 2, theory; \triangle , experiment), and $c = 5 \times 10^{-5}$ mol/L (curve 3, theory; \circ , experiment). Theoretical curves calculated with $D = 5 \times 10^{-6}$ cm²/s, $\omega = 2.28 \times 10^9$ cm²/mol, and $b = 1.69 \times 10^5$ L/mol.

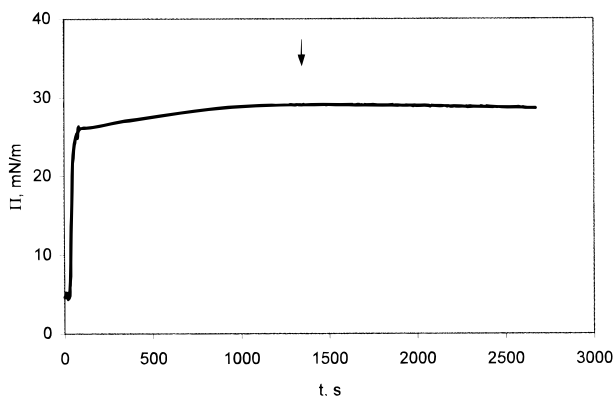


Figure 7. Kinetics of C_{12} DMPO penetration process for $\Theta_2 = 0.35$ and $c = 10^{-4}$ mol/L. The arrow indicates the maximum value of the surface pressure.

lower than the theoretical ones, because eq 4 does not account for the aggregation processes within the monolayer. Therefore, the discrepancy between the theory and the experiment for $\Pi > 15$ mN/m indicates implicitly that within this surface pressure range aggregation occurs in the mixed monolayer. This indication is also supported by the curves of the penetration dynamics for different C_{12} DMPO concentrations shown in Figure 6. For $c \leq 10^{-5}$ mol/L the theoretical and experimental curves of dynamic surface pressure are quite close to one another, while for higher C_{12} DMPO concentrations the experimental Π values are significantly lower than the theoretical ones, that can be explained by the fact that a certain portion of the adsorbed C_{12} DMPO molecules are incorporated within the mixed aggregates. This phenomenon is similar to the effect that accompanies the adsorption of a weakly soluble amphiphile capable for the formation of two-dimensional aggregates within the monolayer at some definite critical value of surface pressure, described recently elsewhere.³¹ For this system the experimental Π - t dependencies exhibit an inflection point at a critical surface pressure value and are characterized by a sharp decrease in the slope of the curve for surface pressure values above the critical value.

An important consequence of the penetration process for high C_{12} DMPO concentration is presented in Figure 7. The dynamic curve has a maximum at $t = 1300$ s and $\Pi \approx 27$ mN/m. It is interesting to note that this surface pressure value coincides with the collapse pressure of the individual C_{20} DMPO monolayer

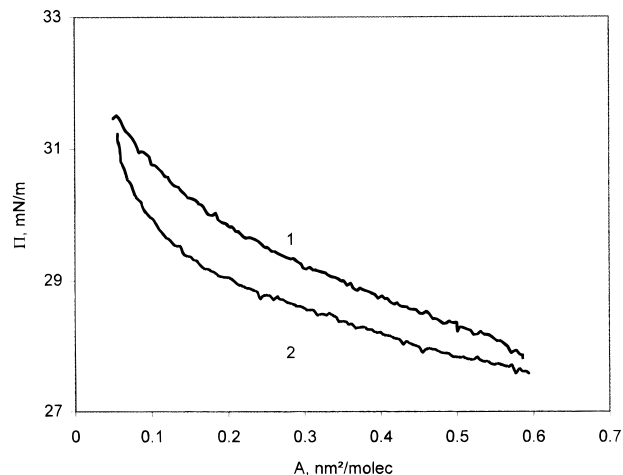


Figure 8. Surface pressure vs area per one C_{20} DMPO molecule isotherm for a mixed monolayer: (curve 1) compression of the monolayer; (curve 2) decompression of the monolayer. The experimental conditions are the same as those for Figure 7.

(Figure 2). Therefore, the decrease in the mixed monolayer pressure for $t > 1300$ s (see Figure 7) indicates that at the same surface pressure, monolayer collapse is induced by the adsorption of soluble surfactant. Subsequent compressions of the monolayer (Figure 8) take place without any peculiar features down to extremely low values of area per C_{20} DMPO molecule, $A_0 = 0.05$ nm²/molecule. At this compression, where for C_{20} DMPO a transition of the two-dimensional monolayer material into three-dimensional phase occurs, the surface pressure exceeds significantly the collapse pressure $\Pi \approx 27$ mN/m. It is obvious that in this case the surface pressure increase is caused by the adsorbed C_{12} DMPO molecules or their interactions with C_{20} DMPO molecules. This is also indicated by the hysteresis loop for decompression/compression of the layer; see Figure 8. The fact that the two branches of the loop are almost closed together shows that the process is reversible, that is, any partial loss of the soluble surfactant during the compression, caused by desorption, is almost entirely compensated by the subsequent adsorption of C_{12} DMPO molecules from the solution during the decompression process.

The conclusion that the formation of aggregates by molecules of soluble C_{12} DMPO with insoluble C_{20} DMPO takes place is additionally supported by the analysis of the mixed monolayer compression isotherms. Such an isotherm for $A_0 = 0.6$ nm²/molecule and $c = 3 \times 10^{-6}$ mol/L is shown in Figure 9. The theoretical calculations were performed according to eq 18 (C_{12} DMPO molecules do not enter the aggregates) and to eq 21 (formation of mixed aggregates). It can be seen that the theoretical model, which assumes the formation of mixed aggregates, leads to a better agreement with the experimental data. Including in the consideration the dependence of the surface concentration of the monomers on the monolayer area according to ref 30, one can transform eqs 18 and 21 into the expressions

$$\Pi = RT \frac{\Gamma_{10}A_0 - (A/A_{2c})^2}{(A - \omega) - \Gamma_{10}A_0\omega} - B \quad (25)$$

and

$$\Pi = RT \frac{(\Gamma_{10}A_0 + 1)(A/A_{2c})^2}{(A - \omega) - \Gamma_{10}A_0\omega} - B \quad (26)$$

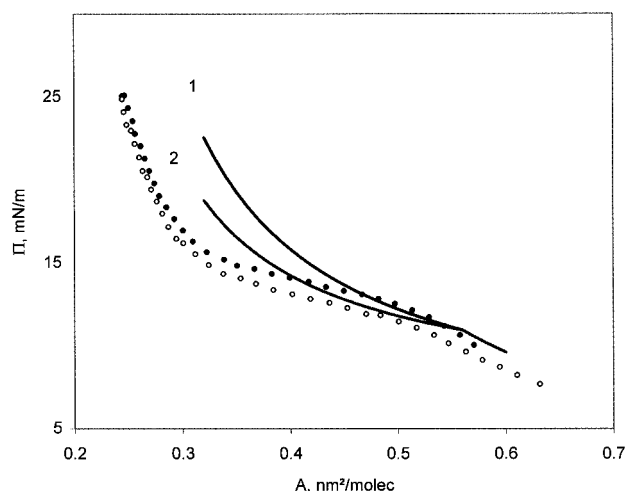


Figure 9. Surface pressure vs area per one $C_{20}DMPO$ molecule isotherm after the penetration ($A_0 = 0.6 \text{ nm}^2/\text{molecule}$, $c = 3 \times 10^{-6} \text{ mol/L}$) for the compression (●) and decompression (○) of the monolayer. Theoretical calculations performed according to eqs 18 and 21 for $\omega = 0.14 \text{ nm}^2/\text{molecule}$, $A_{c2} = 0.56 \text{ nm}^2/\text{molecule}$, and $B = 3.0 \text{ mN/m}$.

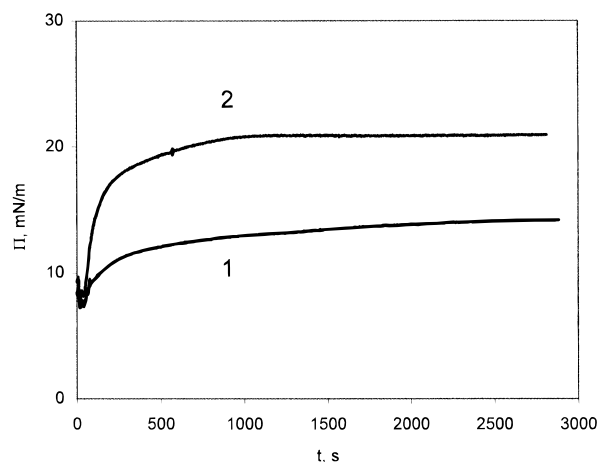


Figure 10. Dynamics of the $C_{12}DMPO$ penetration into a $C_{20}DMPO$ monolayer for $A_0 = 0.35 \text{ nm}^2/\text{molecule}$ and the concentrations 10^{-5} mol/L (curve 1) and $5 \times 10^{-5} \text{ mol/L}$ (curve 2).

respectively. Equation 26 yields perfect agreement between the theory and the experiment for the same values of the main parameters that were used for eq 24 ($\omega = 0.19 \text{ nm}^2/\text{molecule}$ and $B = 7.0 \text{ mN/m}$). In the calculations performed according to eqs 19, 21, and 26, the value $\Gamma_{10}A_0 = 0.3$ was assumed for $A_0 = 0.6 \text{ nm}^2/\text{molecule}$. This corresponds to the value $\Theta_1 = 0.19$, which follows from the adsorption isotherm eq 8. It is obvious that for this $C_{12}DMPO$ concentration, the isotherm eq 5 leads to a similar value $\Theta_1 = 0.22$. Figure 9 shows also the curve for the decompression of the mixed monolayer performed immediately after its compression to $A = 0.22 \text{ nm}^2$, i.e., for the case when no collapse takes place. The difference between the two isotherms does not exceed 1 mN/m , which confirms the assumption used in the theoretical models, namely that no significant desorption of soluble surfactant occurs during the compression of the monolayer.

The dynamic curves that correspond to the penetration of $C_{12}DMPO$ molecules into the two-phase coexistence region of the $C_{20}DMPO$ monolayer at $A_0 = 0.35 \text{ nm}^2/\text{molecule}$ are shown in Figure 10. It can be seen that the values of the equilibrium surface pressure are rather low: 14.5 and 21.5 mN/m for $C_{12}DMPO$ concentrations of 10^{-5} and $5 \times 10^{-5} \text{ mol/L}$, respectively.

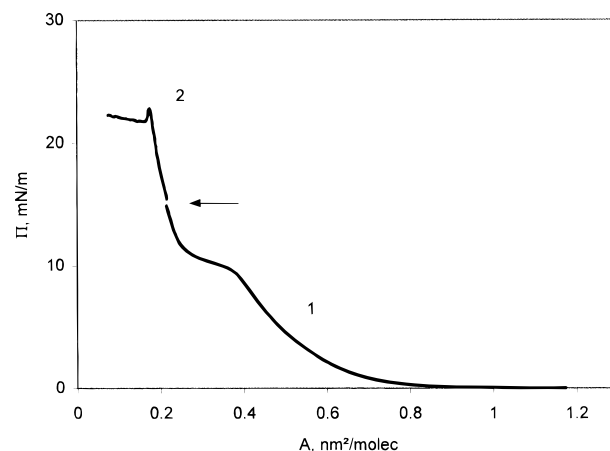


Figure 11. Surface pressure vs area per one $C_{20}DMPO$ molecule isotherm along the interval of individual monolayer compression to $A_0 = 0.23 \text{ nm}^2/\text{molecule}$ (curve 1), and after the penetration of $C_{12}DMPO$ into the monolayer at the concentration 10^{-5} mol/L (curve 2). The arrow indicates the penetration point.

For the case that for the same $C_{12}DMPO$ concentrations no aggregation takes place, eq 4 yields the values $\Pi = 25.3$ and 38.8 mN/m , respectively for $\Theta_2 = 0.6$. The equation of state (eq 20) can be used for explaining this significant discrepancy. In the discussed experiment, the penetration of $C_{12}DMPO$ takes place in the presence of condensed phase aggregates formed by the insoluble $C_{20}DMPO$ amphiphile. It is possible that these aggregates almost completely incorporate the adsorbing surfactant. Therefore, the contribution of $C_{12}DMPO$ monomers can be neglected in eq 20

$$\Pi = RT \frac{\Gamma_{2c}}{1 - \omega(\Gamma_1 + \Gamma_2)} - B \quad (27)$$

The simultaneous solution of this equation and Pethica's eq 8 results in the adsorption isotherm equation for the soluble homologue

$$bc = \left(\frac{\theta_1}{1 - \theta_1 - \theta_2} \right)^{\Theta_{2\bar{n}}/1 - \theta_2} \exp \left[\frac{\theta_1 \Theta_{2\bar{n}}}{(1 - \theta_2)(1 - \theta_1 - \theta_2)} \right] \quad (28)$$

This expression is somewhat different from the adsorption isotherm eq 8, which neglects the 2D aggregation within the monolayer. In a large Θ_2 range and for a given bc value, the adsorption isotherm eq 28 predicts lower Θ_1 values than those that follow from eqs 5 and 8. For the experimental conditions that correspond to Figure 9, eq 5 for the concentrations 10^{-5} and $5 \times 10^{-5} \text{ mol/L}$ yields $\Theta_1 = 0.25$ and 0.36 , respectively, while eq 28 for these concentration values yields $\Theta_1 = 0.16$ and 0.21 , respectively. At these Θ_1 values the calculated data of the equilibrium surface pressure for the mixed monolayer, which were obtained according to eq 27 or 21, agree with the experimental data to within $2\text{--}3 \text{ mN/m}$.

The studies of the penetration into the condensed $C_{20}DMPO$ monolayer at $A_0 = 0.22 \text{ nm}^2/\text{molecule}$ have led to unexpected results. Successive stages of this process are illustrated by Figures 11 and 12. Comparing the isotherm shown in Figure 11 with that reproduced in Figure 2, which characterizes the $C_{20}DMPO$ monolayer without any penetrating component, one can see that even for rather significant bulk concentration, the tightly compressed part of the Π – A isotherm of $C_{20}DMPO$ (curve 2) has not been affected by the penetration of $C_{12}DMPO$.

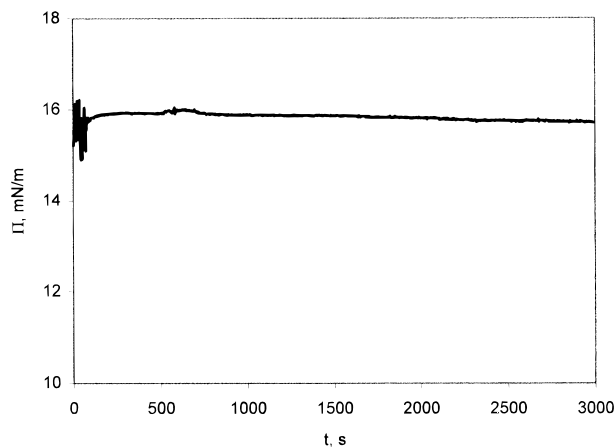


Figure 12. Dynamics of C_{12} DMPO penetration at concentration 10^{-5} mol/L into the C_{20} DMPO monolayer for $A_0 = 0.23$ nm²/molecule.

The increase of the Π value, as predicted from eqs 27 and 28, should amount to a few mN/m. It is seen from Figure 12, however, that the dynamic surface pressure during the penetration process remains nearly the same as for the initial C_{20} DMPO monolayer, i.e., about 16 mN/m. It follows then that the tightly packed C_{20} DMPO monolayer is impenetrable for the adsorbing C_{12} DMPO molecules.

Conclusions

A model system, which consists of the mixed monolayer of an insoluble ($C = 20$) and soluble ($C = 12$) homologue of dimethylalkylphosphine oxide can provide a general basis for a better understanding of the penetration of soluble surfactants into Langmuir monolayers. The fact that the values of the partial molar area of the two homologues are roughly equal to each other, and the adsorption monolayer of soluble surfactant has ideal behavior, has significantly simplified the theoretical analysis of the equilibrium and dynamic behavior of the mixed monolayer.

Theoretical problems concerning the penetration of surfactant dissolved in the substrate, into the Langmuir monolayer, are discussed. This penetration system allows simplification of the theoretical developments, particularly for the case of an ideal (with respect to soluble surfactant) uncharged monolayer, which is composed of homologous amphiphiles having very similar values of the partial molar area. The generalized Szyszkowski–Langmuir equation of state and the generalized Langmuir adsorption isotherm equation can be used to describe equilibrium and dynamics of the penetration process into Langmuir monolayers in the fluidlike state. The experimental data obtained for the mixture of soluble C_{12} DMPO and insoluble C_{20} DMPO were found to agree well with the theoretical predictions based on the characteristics of these amphiphiles as single-component C_{12} -DMPO solutions and C_{20} DMPO monolayers.

The theoretical treatment of the penetrated monolayers, capable of 2D aggregation, is more complicated and was considered within the framework of a generalized Volmer's equation of state. To account for the aggregation of the insoluble homologues in the penetrated monolayers as condensed phase, the quasichemical model of the aggregation equilibrium was applied. Equations of state for a mixed monolayer were derived for different cases, such as the assumptions about the composition of 2D aggregates formed during the penetration or compression of the monolayer. Soluble surfactant adsorption isotherm equations for the tightly packed Langmuir monolayer, either with or without 2D aggregation, were derived from the

simultaneous solution of the corresponding equation of state and Pethica's equation. A mixed aggregates model was found to have the best agreement with the experimental Π – A isotherms and provide a satisfactory agreement between the theoretical and experimental adsorption isotherms.

The theoretical methods developed in this work for the analysis of equilibrium and kinetics of the penetration process, and for the description of equilibrium behavior of mixed monolayers formed thereupon, have the potential to be employed for the studies of more complicated systems. For example, in the case of protein penetration into the two-phase coexistence region of phospholipid monolayers (DPPC, DMPE), the method using reasonable assumptions based on an overall thermodynamic description presented above has to be extended to account for the existence of free charges and multiple states of the adsorbed protein molecule.

Acknowledgment. Financial assistance from the Deutsche Forschungsgemeinschaft (SFB 312 "Vectorial Membrane Processes"), Alexander von Humboldt foundation, the European Community (INCO ERB-IC15-CT96-0809), and the Fonds der Chemischen Industrie is gratefully acknowledged.

References and Notes

- (1) Pethica, B. A. *Trans. Faraday Soc.* **1955**, *51*, 1402.
- (2) Anderson, P. J.; Pethica, B. A. *Trans. Faraday Soc.* **1956**, *52*, 1080.
- (3) Alexander, D. M.; Barnes, G. T. *J. Chem. Soc., Faraday Trans. 1* **1980**, *76*, 118.
- (4) Motomura, K.; Hayami, I.; Aratono, M.; Matuura, R. *J. Colloid Interface Sci.* **1982**, *87*, 333.
- (5) McGregor, M. A.; Barnes, G. T. *J. Colloid Interface Sci.* **1976**, *54*, 439; **1977**, *60*, 408.
- (6) Panaiotov, I.; Ter-Minassian-Saraga, L.; Albrecht, G. *Langmuir* **1985**, *1*, 395.
- (7) Tajima, K.; Koshinuma, M.; Nakamura, A. *Langmuir* **1991**, *7*, 2764.
- (8) Sundaram, S.; Stebe, K. J. *Langmuir* **1996**, *12*, 2028.
- (9) Jiang, Q.; O'Lenick, C. J.; Valentini, J. E.; Chiev, I. C. *Langmuir* **1995**, *11*, 1138.
- (10) Asano, K.; Miyano, K.; Ui, H.; Shimomura, M.; Ohta, I. *Langmuir* **1993**, *9*, 3587.
- (11) Vollhardt, D.; Wittig, M. *Colloids Surf.* **1990**, *47*, 233.
- (12) Siegel, S.; Vollhardt, D. *Colloids Surf. A* **1993**, *76*, 197.
- (13) Hall, D. G. *Langmuir* **1986**, *2*, 804.
- (14) Fainerman, V. B.; Lylyk, S. V. *Kolloidn. Zh.* **1983**, *45*, 500.
- (15) Krotov, V. V. *Kolloidn. Zh.* **1985**, *47*, 1075.
- (16) Fainerman, V. B. *Zh. Fiz. Khim.* **1988**, *62*, 1003.
- (17) Vollhardt, D.; Brezesinski, G.; Makievski, A. V. Manuscript in preparation.
- (18) Fainerman, V. B.; Lucassen-Reynders, E. H.; Miller, R. *Colloids Surf. A*, in press.
- (19) Rusanov, A. I. *Mitselloobrazovanye v rastvorakh poverkhnostno-aktivnykh veshchestv*; Khimya: Sankt-Peterburg, 1992.
- (20) Fainerman, V. B.; Vollhardt, D.; Melzer, V. *J. Phys. Chem.* **1996**, *100*, 15478.
- (21) Ward, A. F. H.; Tordai, L. *J. Chem. Phys.* **1946**, *14*, 453.
- (22) Ziller, M.; Miller, R. *Colloid Polym. Sci.* **1986**, *164*, 611.
- (23) Vollhardt, D.; Czichocki, G.; Rudert, R. *Colloids Surf. A* **1993**, *76*, 217.
- (24) Makievski, A. V.; Grigoriev, D. O. *Colloids Surf. A*, in press.
- (25) Miller, R.; Joos, P.; Fainerman, V. B. *Adv. Colloid Interface Sci.* **1994**, *49*, 249.
- (26) Fainerman, V. B.; Miller, R.; Joos, P. *Colloid Polym. Sci.* **1994**, *272*, 731.
- (27) Miller, R.; Hoffman, A.; Hartman, R.; Schano, K.-H.; Halbig, A. *Adv. Mater.* **1992**, *4*, 370.
- (28) Fainerman, V. B.; Miller, R. *Colloids Surf. A* **1995**, *97*, 65.
- (29) Miller, R.; Schano, K.-H.; Hoffman, A. *Colloids Surf. A* **1994**, *92*, 189.
- (30) Fainerman, V. B.; Vollhardt, D. *J. Phys. Chem.*, in press.
- (31) Fainerman, V. B.; Vollhardt, D.; Melzer, V. *J. Chem. Phys.* **1997**, *107*, 242.